Current Biology, Vol. 13, 1096–1105, July 1, 2003, DOI 10.1016/S0960-9822(03)00420-2

Actomyosin Transports Microtubules and Microtubules Control Actomyosin Recruitment during *Xenopus* Oocyte Wound Healing

Craig A. Mandato[1,3,*] **and William M. Bement**[1,2]
[1]Department of Zoology and
[2]Program in Cellular and Molecular Biology
University of Wisconsin-Madison
Madison, Wisconsin 53706

Summary

Background: Interactions between microtubules and actin filaments (F-actin) are critical for cellular motility processes ranging from directed cell locomotion to cytokinesis. However, the cellular bases of these interactions remain poorly understood. We have analyzed the role of microtubules in generation of a contractile array comprised of F-actin and myosin-2 that forms around wounds made in *Xenopus* oocytes.
Results: After wounding, microtubules are transported to the wound edge in association with F-actin that is itself recruited to wound borders via actomyosin-powered cortical flow. This transport generates sufficient force to buckle and break microtubules at the wound edge. Transport is complemented by local microtubule assembly around wound borders. The region of microtubule breakage and assembly coincides with a zone of actin assembly, and perturbation of the microtubule cytoskeleton disrupts this zone as well as local recruitment of the Arp2/3 complex and myosin-2.
Conclusions: The results reveal transport of microtubules in association with F-actin that is pulled to wound borders via actomyosin-based contraction. Microtubules, in turn, focus zones of actin assembly and myosin-2 recruitment at the wound border. Thus, wounding triggers the formation of a spatially coordinated feedback loop in which transport and assembly of microtubules maintains actin and myosin-2 in close proximity to the closing contractile array. These results are surprisingly reminiscent of recent findings in locomoting cells, suggesting that similar feedback interactions may be generally employed in a variety of fundamental cell motility processes.

Introduction

Interactions between the microtubule and F-actin cytoskeletons are critical for many cellular processes, including cell locomotion [1], cell adhesion [2], axon branching [3], and cytokinesis [4]. However, the complexity of these two cytoskeletal systems and the complexity of the processes they control have long frustrated efforts to analyze their mutual dependence. In particular, the abundance and dynamic nature of microtubules and F-actin pose a serious challenge to efforts to distinguish between real and fortuitous interactions between the two systems. Similarly, the diverse array of cellular inputs necessary to accomplish directed cell movement and cytokinesis greatly complicates efforts to tease apart the individual and interdependent contributions made by microtubules and F-actin during these processes.

In spite of these challenges, recent work has identified several potential mechanisms by which microtubules and the actomyosin cytoskeleton may interact. The first of these mechanisms is indirect and is thought to result from microtubule-dependent regulation of myosin-2 contractility and actin polymerization. Specifically, microtubule depolymerization increases actomyosin-based contractility in a variety of different systems [5–8]. Conversely, microtubule polymerization controls actin polymerization-dependent processes such as cell protrusion [9–11].

The second mechanism is via physical association and transport. Evidence for physical association between microtubules and the F-actin cytoskeleton comes from colocalization of microtubules and F-actin in fixed cells [12], cell-free extracts [13], and microtubule-dependent reorganization of F-actin and myosin-2 during cellularization in *Drosophila* embryos [14]. Force/transport interactions between the two systems have also been suggested by actomyosin-dependent control of microtubule movement and dynamics in living cells [15, 16] and by studies of cellular "tensegrity" [17] and have been directly observed in cell-free extracts [18] and locomoting cells [19, 20].

Thus, distinct mechanisms of microtubule-F-actin interaction could potentially occur during a particular cellular motility process. Here we have characterized microtubule-F-actin interactions in wounded *Xenopus* oocytes. Wounding triggers microtubule-modulated formation and closure of an actomyosin array around wounds [21] in a manner analogous to other actomyosin-based contractile processes ranging from cytokinesis to morphogenesis [22, 23]. The actomyosin array develops as the result of both myosin-powered cortical flow of stable F-actin cables toward the wound, where they assemble with myosin-2 into a contractile ring, and the formation of a zone of actin and myosin-2 polymerization around the wound [24]. Using this system, we provide direct evidence for F-actin-microtubule transport interactions, as well as microtubule-dependent control of the zone of polymerization.

Results

Microtubule Reorganization during Oocyte Wound Healing

The *Xenopus* oocyte microtubule cytoskeleton is unusually stable [25, 26] and contains numerous cortical microtubules [27]. We first characterized the distributions of microtubules, F-actin, and myosin-2 in wounded oocytes by triple labeling fixed samples. Microtubules formed a radial array around wounds, and both F-actin

*Correspondence: camandato@facstaff.wisc.edu
[3]After July 1, 2003: Department of Anatomy and Cell Biology, Strathcona Anatomy and Dentistry Bldg, McGill University, 3640 University Street, Montreal, PQ, Canada H3A 2B2.

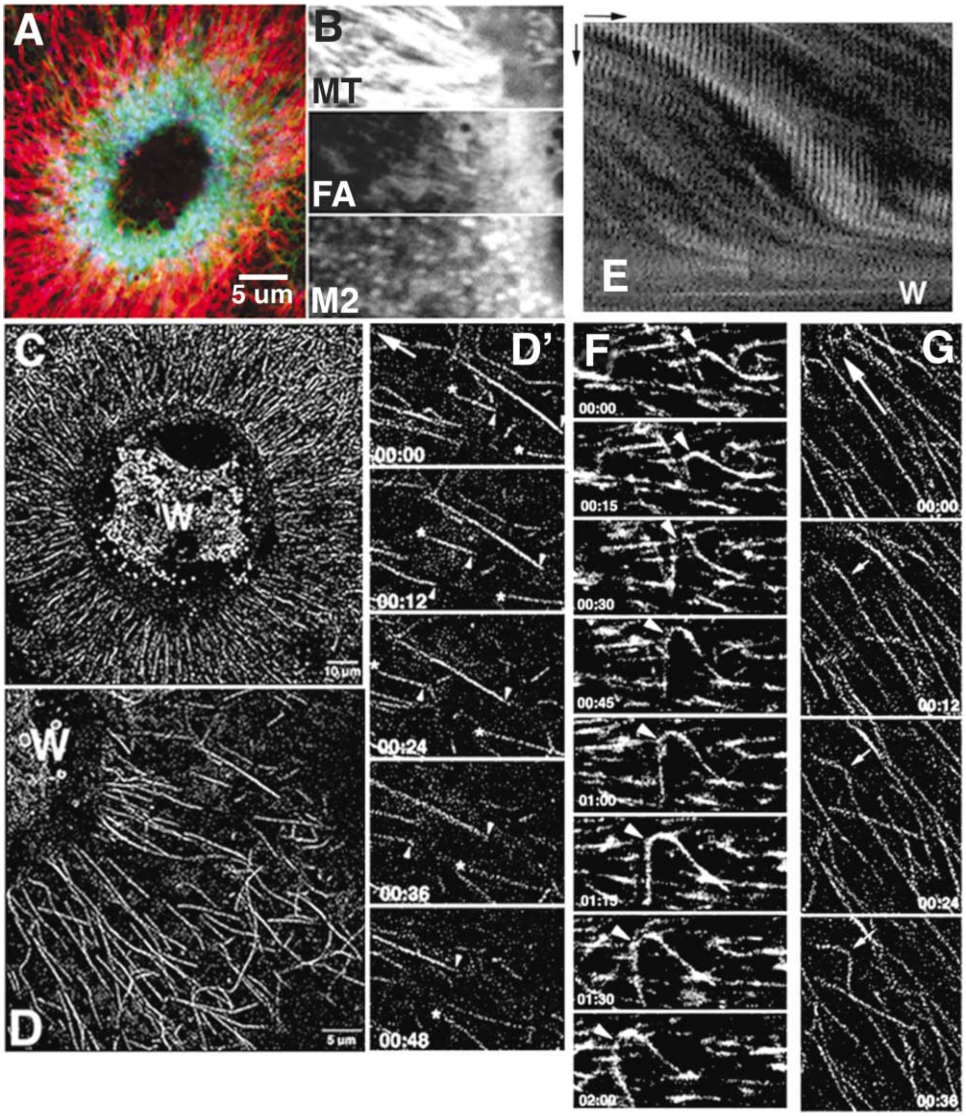

Figure 1. Microtubule Organization around Wound Borders

All times are in min:sec.

(A) Confocal image of a laser-wounded oocyte. Microtubules (red), F-actin (green), and myosin-2 (blue) show complementary distribution around the wound.

(B) Individual channels (MT, microtubule; FA, F-actin; and M2, myosin-2). F-actin and myosin-2 concentrate inside the area of highest microtubule density.

(C) Image from a movie of an OG-Tax-injected oocyte. Microtubules are organized into a radial array around the wound (W). See Movie 1 (Movies are available in the Supplemental Data available with this article on line).

(D) Image from a movie of a wound in an OG-Tax-injected oocyte. Microtubules are perpendicular to the wound border and translocate to the wound. See Movie 2.

(D′) Time course of microtubule movement toward the wound (indicated by an arrow). Asterisks mark the leading ends of individual microtubules, and arrowheads mark the trailing ends.

(E) Kymograph of OG-Tax-labeled microtubule motility toward the wound edge. Horizontal arrow is 45 s; vertical arrow is 5 μm. Microtubules accelerate as they approach the wound border (w), then slow at its immediate edge.

(F) Images from a movie of an OG-Tax-injected oocyte. An arrowhead shows a sharply bent microtubule moving toward the wound.

(G) Images from a movie of an OG-Tax-injected oocyte. Microtubules buckle (arrowhead) at the wound border. The arrow indicates direction of flow.

and myosin-2 were concentrated just inside this array, in a region flanked by microtubule ends (Figures 1A and 1B). Quantification showed that microtubule ends were more than four times as abundant at wound edges than in regions greater than 10 μm distal to the wounds (4.5 $\pm$ 0.8; mean $\pm$ SEM; $p < 0.5$).

To label cortical microtubules in living samples, we microinjected oocytes with 100 nM (final) Oregon Green-488 taxol (OG-Tax). This probe binds to microtubules specifically, but with lower affinity than unlabeled taxol [28], and has been successfully used for following the reorganization of spindle microtubules during mitosis in

Table 1. Translocation and Polymerization Rates of Microtubules in Laser-Wounded *Xenopus* Oocytes

Measurement (μm/min)	Rate[a]	Range	Events Measured	Individual Measurements	Independent Experiment
Microtubule translocation (coinjected with G-actin)	2.68 ± 0.76	1.92–4.24	45	302	9
Microtubule translocation (coinjected with phalloidin)	2.46 ± 0.32	2.07–3.06	42	299	8
F-actin (phalloidin)	2.77 ± 0.60	2.15–3.91	33	337	7
Microtubule translocation (Lat B pretreatment)	0.577 ± 0.21	0.47–0.71	15	110	3
Microtubule translocation (WGA pretreatment)	0.322 ± 0.09	0.65–0.19	18	134	4
Microtubule polymerization	11.18 ± 1.01[b]	26.94–8.40	25	226	7
Microtubule depolymerization	33.12 ± 4.16	41.40–15.60	13	94	6

[a] Rates are expressed as mean ± S.D.
[b] Corrected for local flow rates.

living cultured cells [29]. OG-Tax at 100 nM did not significantly impact the oocyte microtubule cytoskeleton (see Supplemental Data available with this article online).

OG-tax-injected oocytes were laser wounded and imaged by time-lapse, confocal microscopy as previously described [24]. Microtubules reorganized into a radial array after wounding, at least in part because they translocated to the wound border (Figures 1C, 1D, and 1D′; Movies 1 and 2 [see Supplemental Data]). Kymograph analysis demonstrated that microtubules accelerated as they approached the wound border and then decreased in speed upon reaching the wound edge (Figure 1E). Microtubules moved at a mean rate of 2.68 μm/min (Table 1), predominantly parallel to their long axes (87% out of 3304 microtubules observed; see also Figures 1C and 1E; Movies 1 and 2). However, some (13%) microtubules translocated toward wounds in a bent manner (Figure 1F), demonstrating that movement was via translocation rather than treadmilling (e.g., [30]). It was also found that, upon reaching the edge of the wound, microtubules buckled and kinked (Figure 1G).

Microtubules Are Transported via Association with F-Actin Cables

To test whether microtubule translocation was actin dependent, we wounded oocytes and then treated them with latrunculin, to depolymerize actin. Latrunculin treatment resulted in cessation of microtubule translocation toward the wound (Figures 2A and 2B; Movie 3) and microtubule buckling (not shown). Furthermore, pretreatment of oocytes with latrunculin prevented microtubule translocation after wounding (Table 1; Movie 4; see also Supplemental Data), as did pretreatment with wheat germ agglutinin (Table 1), which freezes actomyosin-based cortical flow without depolymerizing actin [7, 24].

Actin-dependent microtubule transport could result from physical attachment of microtubules to translocating F-actin or from nonspecific transport via cortical flow sweeping the microtubules to the wound border. Dual-label analysis of oocytes injected with both OG-tax and Alexa 568-phalloidin (AX-Ph), a marker for stable F-actin [24], revealed that translocating microtubules were associated with translocating F-actin cables (Figures 2C, 2C′, and 2D; Movies 4–6). At higher magnification it was clear that most microtubules (79.56%; 2871 microtubules monitored) had associated F-actin (Figures 2C′, 2D, and 2E; Movies 5 and 6). Such associations were manifest as side-to-side alignment or overlap and end-to-end contact (Figures 2C and 2D; Movies 4–6). In samples where the packing of actin cables and microtubules was not too dense, the leading ends of microtubules were seen to move in clear spatial and temporal synchrony with associated actin filament cables (Figure 2C; Movie 6).

Several other findings confirmed that microtubules were transported by F-actin. First, of those microtubules displaying bends as they move, 89% bent away from the direction of flow at points where contact with F-actin terminated or where they made contact with a second, adjacent actin cable (Figure 3A). Second, F-actin often associated in an end-on manner with two or more microtubules that splayed out behind as if being dragged by the F-actin aggregate (Figure 3B; Movie 7). Third, microtubules near the wound edge buckled and broke when F-actin associated with their trailing ends moved more quickly than the F-actin associated with their leading ends (Figure 3C; Movie 8). Fourth, the degree of F-actin microtubule colocalization observed in the region of transport was significantly higher than would be expected based on colocalization resulting from tighter packing of the two polymers as they approached the wound border (Figure 3D; see Experimental Procedures for details). Finally, dual-label kymograph analysis revealed a tight spatiotemporal correlation between accelerating F-actin and accelerating microtubules (Figure 3E).

The Zone of Actin Polymerization Is the Site of Microtubule Buckling and Assembly

Actin accumulates around wounds as a result of both contraction-based cortical flow and formation of a zone of actin and myosin-2 assembly around wounds [24]. To assess potential roles for microtubules in the assembly zone, we injected oocytes with both OG-Tax and Alexa-568 G-actin (AX-actin), which acts as a marker for the dynamic F-actin. The zone of actin polymerization, characterized by formation of transient, actin-rich protru-

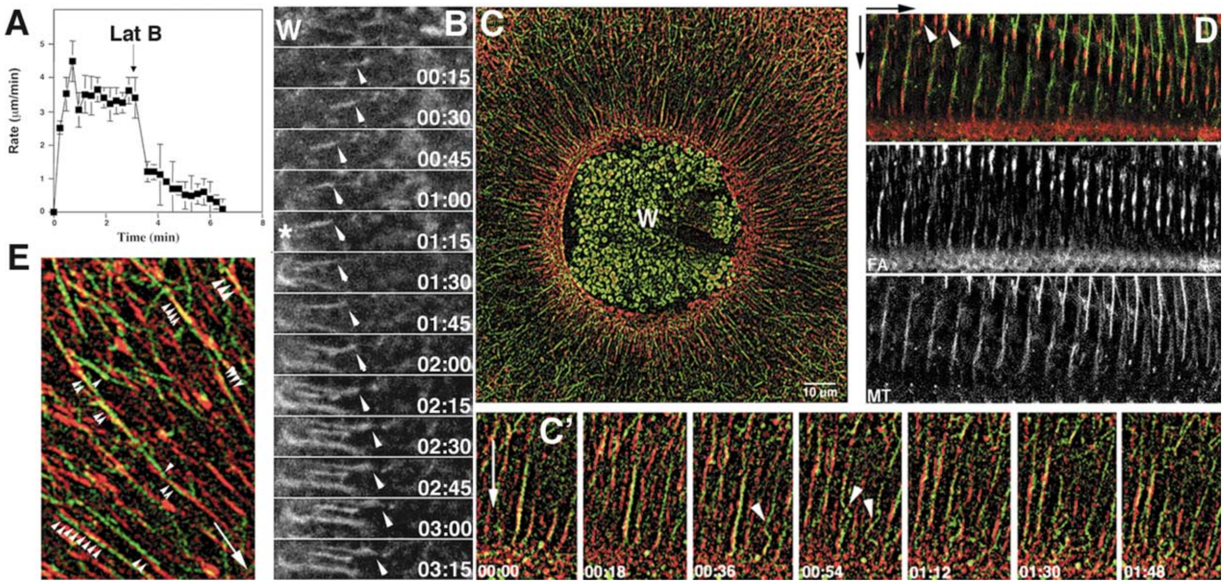

Figure 2. Microtubule Transport is F-Actin Dependent

(A) Plot of instantaneous rates of microtubules before and after treatment with latrunculin B (20 μM). Microtubule translocation to the wound border was arrested after latrunculin treatment. For each point, the rates of movement of a minimum of 10 microtubules were quantified; bars indicate standard error of the mean (SEM).

(B) Images from a movie of an OG-Tax-injected oocyte. Arrowheads show a microtubule translocating to the wound (W), until latrunclin application (asterisk). See Movie 3.

(C) Double-labeled image from a movie of an oocyte injected with OG-Tax (green) and Alexa 568-phalloidin (red). See Movie 5.

(C′) Microtubules move to the wound (arrow) in association with F-actin and buckle upon reaching the wound edge (arrowheads). See Movie 6.

(D) Dual-label images showing end-end association between F-actin (FA, red) and microtubules (MT, green); the overlap of the two is indicated in two frames by arrowheads. F-actin is localized to the tip of microtubules moving to the wound. The horizontal arrow is 30 s; the vertical arrow is 15 μm. See Movie 7.

(E) Dual-label image from a movie showing microtubules (green) aligned with F-actin (red; alignment indicated by arrowheads).

sions and actin comets, coincided with the region where the ends of translocating microtubules started buckling at the cortex (Figures 4A–4C; Movie 9).

Efforts to visualize dynamic microtubules by injection of fluorescent tubulin were unsuccessful (see Supplemental Data). We therefore generated and expressed a fusion of eGFP with a *Xenopus* oocyte α-tubulin isoform [31]. This construct (eGFP-Xtub) incorporated into meiotic spindles (see Supplemental Data) but only poorly incorporated into cortical microtubules, even after three days of expression. Remarkably, however, after wounding, eGFP-Xtub-labeled, dynamic microtubules formed in a zone restricted to the region around the wound borders (Figures 4D and 4E; Movies 10 and 11). These microtubules displayed assembly and disassembly rates similar to those observed in other systems (Table 1). Analysis of microtubule orientation, based on rapid assembly from the plus end, revealed that 20% of the dynamic microtubules were oriented with their plus ends facing the wound (within a 90° arc), 50% were oriented with their minus ends facing the wound (within a 90° arc), and the remaining 30% were oriented perpendicular to the wound. However, these numbers necessarily underreport microtubules with plus ends facing the wound because most plus end facing microtubules close to the wound would be pulled into the wound before assembly could be detected.

Microtubules polymerizing away from the wound border appeared to do so more slowly than those polymerizing toward wound borders, but this variation disappeared upon correction for cortical flow. There was, however, a regional effect with respect to assembly in that polymerization rates (after correction for flow) were inversely proportional to the distance from the wound (Figure 4F). Furthermore, the frequency of microtubule polymerization events and the position of the actin assembly zone were also correlated (Figure 4G), as observed above for microtubule buckling events, suggesting that local microtubule assembly/disassembly might contribute to local actin assembly. Local microtubule assembly was not absolutely dependent on cortical flow because eGFP-Xtub-labeled microtubules accumulated around wounds in the presence of latrunculin, although in contrast to controls, the arrays are not radial (Figure 4H).

Microtubules Control the Zone of Actin Assembly Around Wounds

The spatial correlation between assembling and buckling microtubules and dynamic actin suggested that microtubules might regulate the zone of actin assembly. To test this idea, we injected oocytes with Oregon Green-actin (OG-actin), preincubated them in nocodazole to disassemble microtubules, and then wounded them. In nocodazole-treated cells, the zone of actin assembly was broader and less stable than in controls (Figure 5A; Movies 12 and 13), suggesting that microtu-

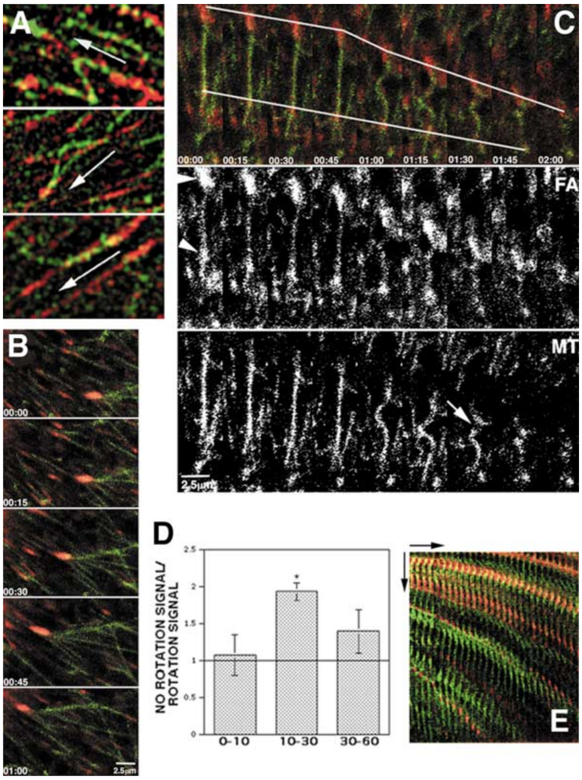

Figure 3. Cotransport of F-Actin and Microtubules

(A) Dual-label images showing examples of bent microtubules. Arrows indicate direction of movement. Microtubules (green) bend away from the direction of movement where they are not associated with F-actin (red).

(B) Images from a movie showing F-actin (red) and microtubules (green). F-actin appears to link the ends of several microtubules and drag them through the cortex. See Movie 8.

(C) Dual-label and split-channel images showing buckling and breakage of a microtubule that is associated with F-actin at both its leading and trailing edges. F-actin at the trailing edge accelerates between the 00:45 and 01:00 time points, whereas the F-actin at the leading edge does not (white lines). Microtubule buckling is observed in precisely this time window. Later (at 01:30), the microtubule breaks (arrow). See Movie 9.

(D) Quantification of specific microtubule-F-actin overlap (see Supplemental Data for details). The ratio of yellow pixels in unrotated: rotated images is significantly higher in the region where microtubule-F-actin cotransport occurs (10–30 μm) than at the wound edge (0–10 μm) or in areas more than 30 μm away from wound. Results are mean ± SEM from four independent experiments; an asterisk indicates < 0.01.

(E) Double-labeled kymograph. F-actin (red) and microtubules (green) show same patterns of acceleration and deceleration. W indicates the wound; the horizontal arrow is 90 s; the vertical arrow is 10 μm.

bules focus the zone of actin polymerization around the wound edge.

Taxol pretreatment, which increases microtubule density and changes the organization of microtubules in this system [7], resulted in broadening of the actin array around wounds (Figure 5B) and/or formation of two rings of actin around wounds. The first of these bordered the wound edge, and the second formed a concentric ring 5–20 μm distal to the first (Figures 5A and 5B; Movie 14). Analysis of fixed samples revealed that taxol treatment caused microtubules to form concentric arrays of bundles around the wound (Figure 5B).

We also examined the effects of taxol treatment on the distribution of the Arp2/3 complex, which normally accumulates around wounds [24]. Taxol treatment significantly increased the width of the region occupied by p16, a conserved component of the Arp2/3 complex [32] (Figure 6A). Furthermore, taxol treatment also resulted in broadening or splitting of the zone of myosin recruitment around wounds (Figure 6B).

The observed defocusing of actin, p16, and myosin-2 from the wound edge suggested that taxol might inhibit closure of the actomyosin array by uncoupling the assembly zone from the contractile ring. To test this possibility, we injected oocytes with Oregon Green phalloidin, a marker for stable F-actin and the contractile ring, and AX-actin, a marker for the assembly zone [24], treated them with taxol, and then wounded them. In control oocytes, the assembly zone remained tightly associated with the contractile ring (Figure 6C; Movie 15). However, in taxol-treated oocytes, actin assembly was concentrated in the outer ring, 5–10 um displaced from the contractile ring (Figure 6C; Movie 16). Thus, microtubules coordinate the zone of assembly with the contractile ring around the wound edge.

Discussion

The results of this study demonstrate directly the existence and importance of interplay between microtubules and the transient contractile array of F-actin and myosin-2 that assembles and closes around *Xenopus* oocyte wounds. Both transport and polymerization interactions between the two systems are evident, and both contribute to assembly and closure of transient contractile rings. These findings are not only intrinsically fascinating but are also directly relevant to other fundamental cellular processes known to be dependent on dynamic microtubule-actomyosin interactions.

Transport

It was previously shown that stable F-actin is pulled to wound borders by the action of a myosin, presumably myosin-2, that localizes at the edge of the wound [24]. In this report, we found that the translocating F-actin associates with and transports microtubules to the wound border. Thus, microtubule transport is ultimately powered by actomyosin-based contraction. The demonstration of F-actin-dependent microtubule transport confirms our earlier studies in *Xenopus* egg extracts [13, 18], but there is the obvious difference that in extracts, microtubule-dependent actin translocation was observed, whereas here actin-dependent microtubule translocation was observed. The simplest explanation for this difference is that in extracts F-actin is unanchored, whereas in oocytes it is tightly integrated into the cortex [7]. The transport of microtubules by F-actin also confirms recent studies of "tensegrity"; these studies show that experimental displacement of the actin cytoskeleton results in a corresponding displacement of microtubule-associated organelles [17].

Transport of microtubules by translocating F-actin

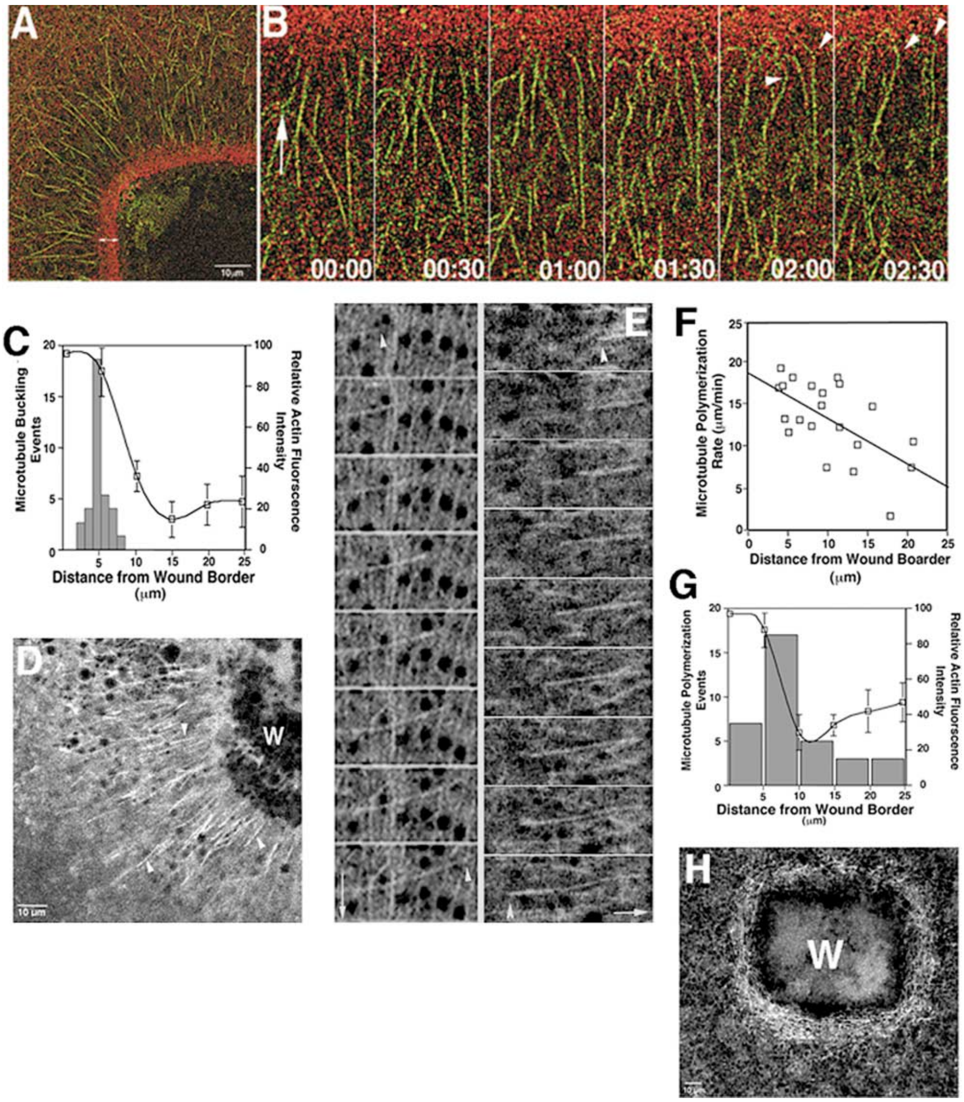

Figure 4. Local Actin Assembly Coincides with Microtubule Breakage and Assembly

(A) Image from a movie of an oocyte injected with OG-taxol and Alexa 568 G-actin. Microtubules (green) move to the zone of actin polymerization (red; indicated by a double-headed arrow). Microtubule disappearance into the zone is correlated with bending and buckling. See Movie 10.
(B) Dual-label image from a movie showing microtubules translocating toward the wound (an arrow indicates the direction of the wound). Arrowheads show individual microtubules buckling.
(C) Plot of microtubule buckling and relative actin intensity versus distance from the wound border. Microtubule buckling is most common near the actin assembly zone.
(D) Image showing e-GFP-Xtub-labeled microtubules (arrowheads) near the wound.
(E) Images from a movie of an oocyte injected with e-GFP-Xtub. Microtubules polymerize perpendicular to (left panels) and away from the wound (right panels). Arrows indicate the direction of flow; arrowheads show the start and stop of polymerization; frames are shown at 4 s intervals. See Movies 11 and 12.
(F) Graph showing that microtubule polymerization rates are inversely correlated with distance from the wound.
(G) Plot of microtubule polymerization events and relative actin intensity versus distance from the wound border. Microtubule assembly events are most common near the zone of actin assembly.
(H) Image from a movie of an oocyte wounded after injection with e-GFP-X tub and treated with latrunculin B (20 μM). Microtubules accumulate around the wound border.

also has important biochemical implications. Specifically, progressive alignment of F-actin and microtubules moving to the wound edge implies that, within the context of a cell, the process of movement itself must be considered an important contributor to biochemical interactions between the two systems. That is, cortical flow promotes alignment of F-actin cables and microtubules, which presumably promotes crosslinking of the two systems. As previously suggested [33], low-affinity crosslinking interactions between microtubules and F-actin may be biologically important because each polymer has the potential to bind multiple crosslinkers. The existence of motility-dependent alignment further underscores this notion, as well as its implication—

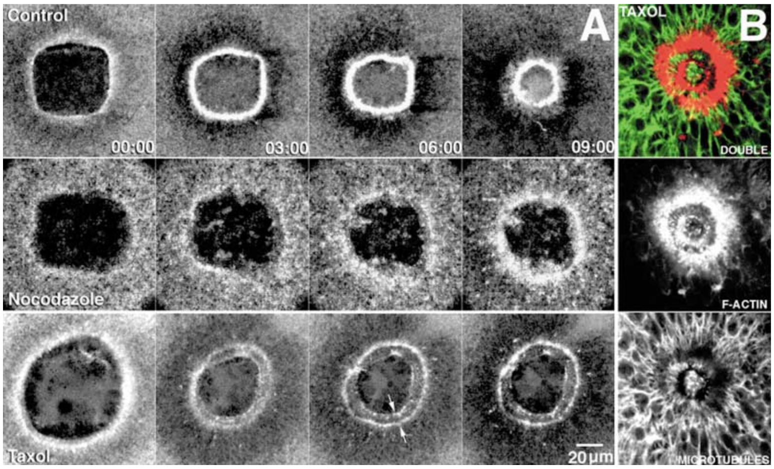

Figure 5. Microtubule Perturbation Defocuses the Actin Assembly Zone.

(A) Images from movies of oocytes injected with OG-actin and wounded after no treatment (control), nocodazole treatment (Nocodazole; 5 μm; 1 hr), or taxol treatment (Taxol; 20 μm; 1 hr). In controls, the zone of F-actin polymerization remains tightly focused around wounds; in nocodazole-treated oocytes it becomes uneven and broadens; in taxol-treated samples it spreads and then splits into two rings (arrows). See Movies 13, 14, and 15.

(B) Confocal fluorescence images showing distribution of F-actin (red) and microtubules (green) in a taxol-treated oocyte subjected to wounding. The microtubule and actin arrays have split into concentric rings.

namely, that a given crosslinker should be given serious consideration even if its measured affinity for F-actin, microtubules, or both is considered low by more traditional standards.

Polymerization

In addition to transport interactions, this work also reveals important features of local assembly interactions—microtubule-dependent control of zones of actin and myosin-2 assembly and the existence of a zone of tubulin polymerization around wound borders. Control of local actin polymerization by microtubules is consistent with previous results from locomoting cells (see [1] for review). However, the results here not only show that microtubules also control local actin assembly during a contractile process, but they also demonstrate that microtubules control local recruitment of myosin-2 and the Arp2/3 complex. Furthermore, the results obtained after microtubule perturbation directly demonstrate the importance of microtubule-dependent control of actin and myosin-2 assembly for the function of a contractile structure. Specifically, the zones of actin and myosin-2 assembly become spatially uncoupled from the contractile ring at the wound edge after microtubule perturbation, showing that microtubules dictate where the contractile array is assembled by regulating local actin and myosin-2 assembly. The concentric rings of actin that form after taxol treatment are particularly striking. The fact that the outer actin array moves away from the wound edge implies that it cannot simply be due to physical occlusion of array closure but instead argues that microtubules control local actin and myosin assembly either via transport or via signaling interactions.

Local microtubule assembly around wounds was completely unexpected because numerous previous studies have shown that although microtubule polymerization in activated *Xenopus* eggs and egg extracts is robust, polymerization in oocytes and oocyte extracts is virtually undetectable [25, 26, 34]. A restricted zone of microtubule polymerization induced by wounding is even more surprising in that although spontaneous microtubule polymerization is observed in a variety of cellular contexts (e.g., [35]), this is, to the best of our knowledge, the first demonstration that local tubulin polymerization can be triggered by an exogenous stimulus. From the biological perspective, however, local assembly after wounding makes good sense in that it provides, complementary to microtubule transport, an alternative source of microtubules at the wound edge.

Model

The findings suggest a working model in which transport and polymerization interactions between microtubules and actomyosin form a spatially coordinated feedback loop initiated by wounding (Figure 7). First, based on previous work [24], wounding results in the establishment of zones of actin and myosin-2 assembly. The initial assembly of actin and myosin-2 at the wound border may be independent of microtubules because we have been unable to prevent it by nocodazole treatment; however, it remains possible that more extreme measures to eliminate microtubules might likewise prevent local actomyosin accumulation. Certainly, both intuition and the quantification of microtubule ends at wound borders suggests that wounding itself generates numerous free microtubule ends that could promote microtubule assembly and thereby promote local actin assembly.

Next, myosin-based contractility drives cortical flow of stable F-actin to the wound [24]. The flowing F-actin is physically associated with microtubules and therefore transports them to the wound edge, where they are buckled and broken by actomyosin-based contractility. This increases the number of microtubule ends at the wound border, which in turn keeps actin and myosin-2 assembly focused near the wound edge, where it is needed. The actomyosin-based transport of microtubules to the wound border is complemented by local microtubule assembly that is independently triggered by wounding. The net result is that as the contractile ring moves forward, so do translocating and newly-assembled microtubules, ensuring that the zones of assembly remains spatially associated with the contractile ring (Figure 7).

Are the current findings peculiar to the oocyte system? Clearly not. It was recently reported that F-actin associates with and transports microtubules away from the leading edge of growth cones [19] and newt lung

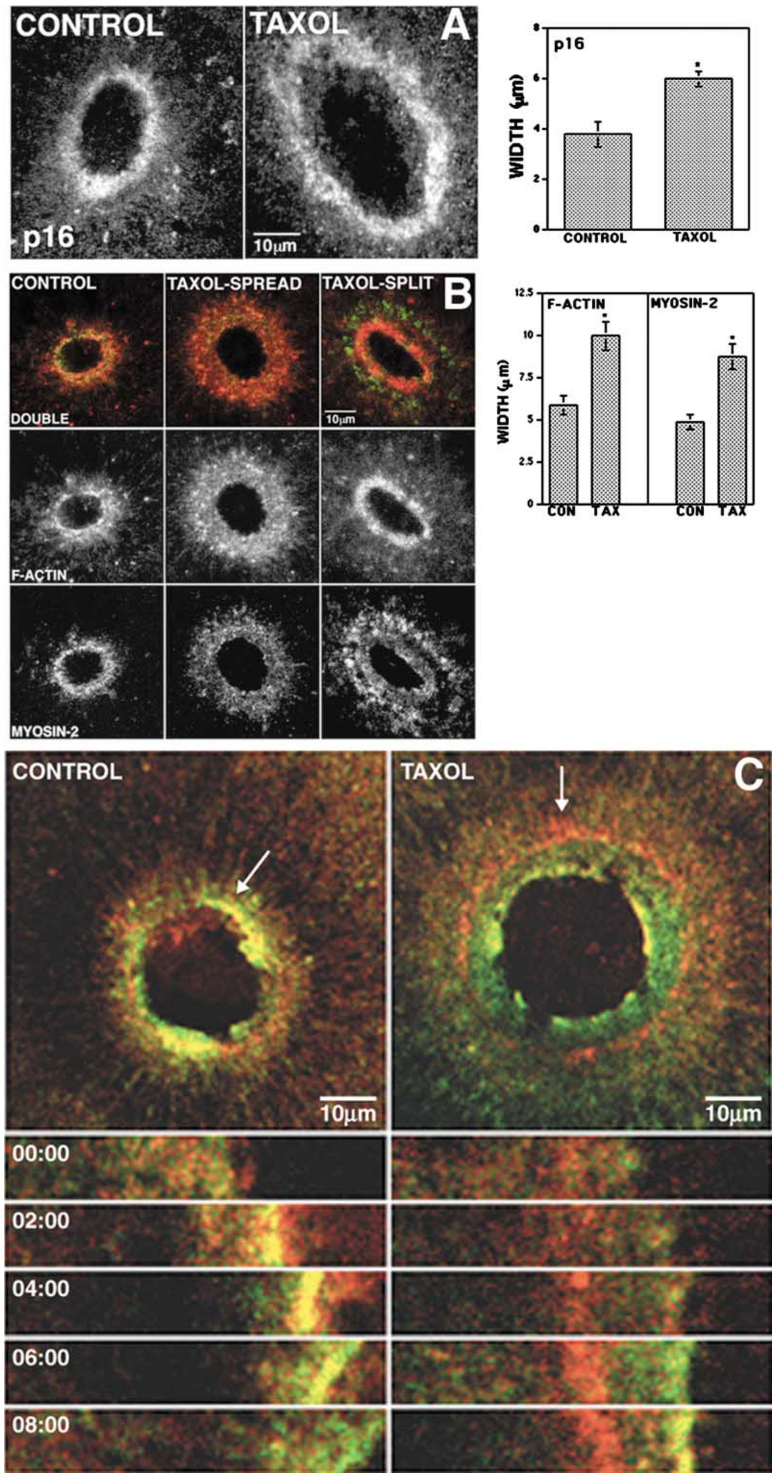

Figure 6. Microtubule Perturbation Disrupts Normal Patterns of Arp2/3 Complex and Myosin-2 Localization and Uncouples the Zone of Actin Polymerization from the Contractile Ring

(A) Confocal images showing distribution of p16 around wounds in control and taxol-treated oocytes. The region of p16 accumulation is broader in the taxol sample. Quantification shows that the width of the region enriched in p16 increases in the presence of taxol. Results are mean ± SEM from three independent experiments; an asterisk indicates $p < 0.01$.

(B) Confocal images showing examples of taxol-induced spreading (Taxol-Spread) or splitting (Taxol-Split) of the region of myosin-2 enrichment around wounds and, for comparison, controls. Quantification shows that the width of the region enriched in actin and myosin-2 around wounds increased in the presence of taxol. Results are mean ± SEM from three independent experiments; an asterisk indicates $p < 0.01$.

(C) Double-labeled images from 4D movies of oocytes injected with Alexa 568-G-actin and OG-phalloidin, treated with taxol (taxol) or nothing (control), and wounded. Lower panels show images taken from the regions indicated by the arrows in the upper image. In control, the zone of assembly (red) encompasses the contractile ring that contains stable F-actin (green). However, in the taxol sample, dynamic actin moves to the outer ring, whereas stable F-actin remains concentrated at the wound border. See Movies 16 and 17.

fibroblasts [20]. The fact that dynamic microtubule-F-actin interactions normally observed in locomoting cells can be triggered in oocytes is strong evidence that such interactions are universal and need only the appropriate cellular situation or stimulus to be evoked.

It was previously suggested that the wound-healing system is particularly relevant to cytokinesis because it entails rapid assembly of a transient, microtubule-modulated, contractile array [21, 24]. The validity of this idea was strongly supported by the recent demonstration that, like wound arrays, fission yeast cytokinetic rings are assembled via both de novo actin assembly and contraction [36]. To extend the analogy, because the present results demonstrate that microtubules control local zones of actin and myosin-2 assembly around wounds, we propose that microtubules likewise control

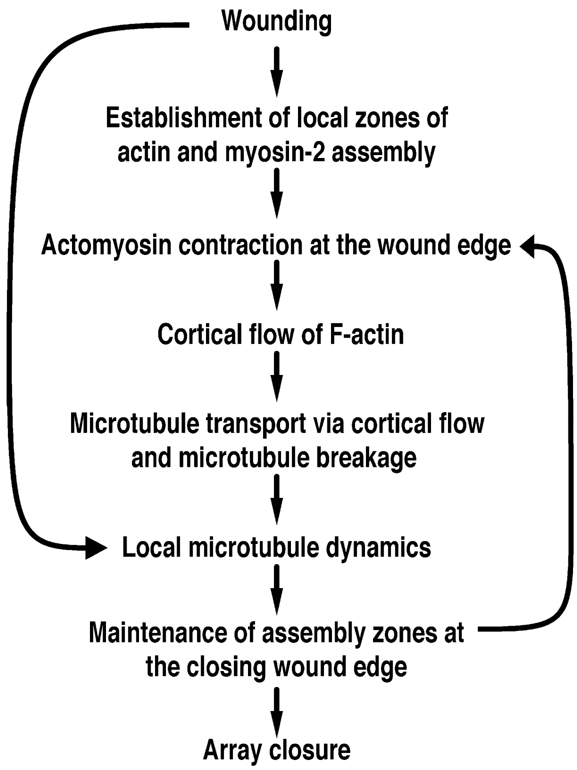

Figure 7. Schematic Diagram of Microtubule-Actomyosin Interactions during Oocyte Wound Healing

zones of local actin and myosin-2 assembly during cytokinesis. This could explain why microtubule disruption during cytokinesis disrupts local patterns of cortical flow [37].

What are the signals that underlie the zones of actin, myosin-2, and microtubule assembly around wounds? The Rho GTPases, Rho, Rac, and Cdc42 are strong candidates in that they have the potential to regulate both the actomyosin and microtubule cytoskeletons [38] and, furthermore, can act as intermediates between the microtubule and actin cytoskeletons (e.g., [39–41]). This concept parallels the proposal that microtubules control local actin and myosin-2 assembly during cytokinesis via local modulation of Rho GTPase activity [4] and is consistent with observations of local segregation of Rac, Rho, and Cdc42 activity around wound edges (H.A. Benink and W.M.B., unpublished data). Although these ideas remain to be tested, the oocyte wound-healing system provides an ideal model for such experiments.

Experimental Procedures

Oocyte Microinjection and Wounding
Oocytes were prepared, injected, and wounded as described in the Supplemental Data. Fluorescent actins and phalloidins were obtained and handled as described in the Supplemental Data. For labeling of dynamic microtubules, the coding region of a *Xenopus* oocyte-specific α-tubulin was amplified by PCR from reverse-transcribed RNA and ligated into a modified pCS2 vector (provided by Anna Sokac, UW-Madison) containing the eGPF upstream of the insertion site. mRNA was transcribed in vivo prior to injection with the SP6 Message Machine (Ambion, Austin, TX).

Fixed-Cell Fluorescence
Cells were fixed and stained for F-actin and myosin-2 as previously described [24]. Microtubules and p16 were labeled as described in the Supplemental Data.

Imaging, Image Processing, and Analysis
4D imaging was performed as previously described [24] with a Biorad 1024 confocal system on a Zeiss axiovert microscope and with the Lasersharp software. The details of this approach are described in the Supplemental Data, as are the details for image processing and analysis.

Quantification of Polymeric Tubulin and Microtubule Ends
Levels of oocyte microtubules were assessed by quantitative immunoblotting as previously described [7] and as discussed in detail in the Supplemental Data. For quantification of microtubule ends, 3D images of fixed samples were generated with the Volocity software (Improvision), and microtubule ends were quantified as described in the Supplemental Data.

Supplemental Data
Supplemental Experimental Procedures, as well as supplemental figures and movies, are available with this article online at http://www.current-biology.com/content/supplemental.

Acknowledgments

We would like to thank the members of our lab for continuous and helpful input. We would also like to thank Bob Adelstein (National Institutes of Health), Dr. Gary Borisy (Northwestern University), Mary Halloran, Jim Pawley, and John Peloquin (University of Wisconsin-Madison) for providing reagents and access to equipment. Many thanks also to Clare Waterman-Storer (Scripps Research Institute) and Paul Forscher (Yale University) for communicating results prior to publication. This work was supported by the National Institutes of Health (GM52932-04A1) and the National Science Foundation (MCB9630860). The National Science Foundation supported the acquisition of the confocal microscope used in this study (NSF9724515 to J. Pawley).

Received: March 20, 2003
Revised: April 22, 2003
Accepted: May 6, 2003
Published: July 1, 2003

References

1. Wittmann, T., and Waterman-Storer, C.M. (2001). Cell motility: can Rho GTPases and microtubules point the way? J. Cell Sci. *114*, 3795–3803.
2. Kaverina, I., Krylyshkina, V., and Small, J.V. (1999). Microtubule targeting of substrate contacts promotes their relaxation and dissociation. J. Cell Biol. *146*, 1033–1044.
3. Dent, E.W., and Kalil, K. (2001). Axon branching requires interactions between dynamic microtubules and actin filaments. J. Neurosci. *21*, 9757–9769.
4. Mandato, C.A., Benink, H.A., and Bement, W.M. (2000). Microtubule-actomyosin interactions in cortical flow and cytokinesis. Cell Motil. Cytoskeleton *45*, 87–92.
5. Danowski, B.A. (1989). Fibroblast contractility and actin organization are stimulated by microtubule inhibitors. J. Cell Sci. *93*, 255–266.
6. Kolodney, M.S., and Elson, E.L. (1995). Contraction due to microtubule disruption is associated with increased phosphorylation of myosin regulatory light chain. Proc. Natl. Acad. Sci. USA *92*, 10252–10256.
7. Canman, J.C., and Bement, W.M. (1997). Microtubules suppress actomyosin-based cortical flow in *Xenopus* oocytes. J. Cell Sci. *110*, 1907–1917.
8. Benink, H.A., Mandato, C.A., and Bement, W.M. (2000). Analysis of cortical flow models in vivo. Mol. Biol. Cell *11*, 2553–2563.
9. Bershadsky, A.D., Vaisberg, E.A., and Vasiliev, J.M. (1991). Pseudopodial activity at the active edge of migrating fibroblast

is decreased after drug-induced microtubule depolymerization. Cell Motil. Cytoskeleton *19*, 152–158.
10. Rosania, G.R., and Swanson, J.A. (1996). Microtubules can modulate pseudopod activity from a distance inside macrophages. Cell Motil. Cytoskeleton *34*, 230–245.
11. Mikhailov, A., and Gundersen, G.G. (1998). Relationship between microtubule dynamics and lamellipodium formation revealed by direct imaging of microtubules in cells treated with nocodazole or taxol. Cell Motil. Cytoskeleton *41*, 325–340.
12. Silverman-Gavrila, R.V., and Forer, A. (2000). Evidence that actin and myosin are involved in the poleward flux of tubulin in metaphase kinetochore microtubules of crane-fly spermatocytes. J. Cell Sci. *113*, 597–609.
13. Sider, J.R., Mandato, C.A., Weber, K.L., Zandy, A.J., Beach, D., Finst, R.J., Skoble, J., and Bement, W.M. (1999). Direct observation of microtubule-f-actin interaction in cell free lysates. J. Cell Sci. *112*, 1947–1956.
14. Foe, V.E., Field, C.M., and Odell, G.M. (2000). Microtubules and mitotic cycle phase modulate spatiotemporal distributions of F-actin and myosin II in *Drosophila* syncytial blastoderm embryos. Development *127*, 1767–1787.
15. Waterman-Storer, C.M., and Salmon, E.D. (1997). Actomyosin-based retrograde flow of microtubules in the lamella of migrating epithelial cells influences microtubule dynamic instability and turnover and is associated with microtubule breakage and treadmilling. J. Cell Biol. *139*, 417–434.
16. Yvon, A.M., Gross, D.J., and Wadsworth, P. (2001). Antagonistic forces generated by myosin II and cytoplasmic dynein regulate microtubule turnover, movement, and organization in interphase cells. Proc. Natl. Acad. Sci. USA *98*, 8656–8661.
17. Wang, N., Naruse, K., Stamenovic, D., Fredberg, J.J., Mijailovich, S.M., Tolic-Norrelykke, I.M., Polte, T., Mannix, R., and Ingber, D.E. (2001). Mechanical behavior in living cells consistent with the tensegrity model. Proc. Natl. Acad. Sci. USA *98*, 7765–7770.
18. Waterman-Storer, C.M., Duey, D.Y., Weber, K.L., Keech, J., Cheney, R.E., Salmon, E.D., and Bement, W.M. (2000). Microtubules remodel actomyosin networks in *Xenopus* egg extracts via two mechanisms of F-actin transport. J. Cell Biol. *150*, 361–376.
19. Salmon, W.C., Adams, M.C., and Waterman-Storer, C.M. (2002). Dual wave-length confocal fluorescent speckle microscopy reveals coupling of microtubules to actin movement in migrating cells. J. Cell Biol. *158*, 31–37.
20. Schaefer, A.W., Kabir, N., and Forscher, P. (2002). Filapodia and transverse retrograde F-actin arcs guide the assembly and transport of two populations of microtubules with unique dynamic parameters in neuronal growth cones. J. Cell Biol. *158*, 139–152.
21. Bement, W.M., Mandato, C.A., and Kirsch, M.N. (1999). Wound-induced assembly and closure of an actomyosin purse string in *Xenopus* oocytes. Curr. Biol. *9*, 579–587.
22. Jacinto, A., Wood, W., Woolner, S., Hiley, C., Turner, L., Wilson, C., Martinez-Arias, A., and Martin, P. (2002). Dynamic analysis of actin cable function during *Drosophila* dorsal closure. Curr. Biol. *12*, 1245–1250.
23. Bement, W.M. (2002). Actomyosin rings: the riddle of the sphincter. Curr. Biol. *12*, R12–14.
24. Mandato, C.A., and Bement, W.M. (2001). Contraction and polymerization to assemble and close actomyosin rings around *Xenopus* oocyte wounds. J. Cell Biol. *154*, 785–797.
25. Heidemann, S.R., and Kirschner, M.W. (1975). Aster formation in eggs of *Xenopus laevis*. Induction by isolated basal bodies. J. Cell Biol. *67*, 105–117.
26. Heidemann, S.R., Hamborg, M.A., Balasz, J.E., and Lindley, S. (1985). Microtubules in immature oocytes of *Xenopus laevis*. J. Cell Sci. *77*, 129–141.
27. Gard, D.L. (1991). Organization, nucleation, and acetylation of microtubules in *Xenopus laevis* oocytes: a study by confocal immunofluorescence microscopy. Dev. Biol. *143*, 346–362.
28. Diaz, J.F., Strobe, R., Engelborghs, Y., Souto, A.A., and Andreu, J.M. (2000). Molecular recognition of taxol by microtubules. Kinetics and thermodynamics of binding of fluorescent taxol derivatives to an exposed site. J. Biol. Chem. *275*, 26265–26276.
29. Evangelio, J.A., Abal, M., Barasoain, I., Souto, A.A., Lillo, M.P., Acuna, A.U., Amat-Guerri, F., and Andreu, J.M. (1998). Fluorescent taxoids as probes of the microtubule cytoskeleton. Cell Motil. Cytoskeleton *39*, 73–90.
30. Rodionov, V.I., and Borisy, G.G. (1997). Microtubule treadmilling *in vivo*. Science *275*, 215–218.
31. Wu, W.L., and Morgan, G.T. (1994). Ovary-specific expression of a gene encoding a divergent alpha-tubulin isotype in *Xenopus*. Differentiation *58*, 9–18.
32. Welch, M.D., DePace, A.H., Verma, S., Iwamatsu, A., and Mitchison, T.J. (1997). The human Arp2/3 complex is composed of evolutionarily conserved subunits and is localized to cellular regions of dynamic actin filament assembly. J. Cell Biol. *138*, 375–384.
33. Selden, S.C., and Pollard, T.D. (1986). Interaction of actin filaments with microtubules is mediated by microtubule-associated proteins and regulated by phosphorylation. Ann. N Y Acad. Sci. *466*, 803–812.
34. Gard, D.L., and Kirschner, M.W. (1987). Microtubule assembly in cytoplasmic extracts of *Xenopus* oocytes and eggs. J. Cell Biol. *105*, 2191–2201.
35. Yvon, A.M., and Wadsworth, P. (1997). Non-centrosomal microtubule formation and measurement of minus end microtubule dynamics in A498 cells. J. Cell Sci. *110*, 2391–2401.
36. Pelham, R.J., and Chang, F. (2002). Actin dynamics in the contractile ring during cytokinesis in fission yeast. Nature *419*, 82–86.
37. Fishkind, D.J., and Wang, Y.L. (1995). New horizons for cytokinesis. Curr. Opin. Cell Biol. *7*, 23–31.
38. Etienne-Manneville, S., and Hall, A. (2002). Rho GTPases in cell biology. Nature *420*, 629–635.
39. Waterman-Storer, C.M., Worthylake, R.A., Liu, B.P., Burridge, K., and Salmon, E.D. (1999). Microtubule growth activates Rac1 to promote lamellipodial protrusion in fibroblasts. Nat. Cell Biol. *1*, 45–49.
40. Ren, X.D., Kiosses, W.B., and Schwartz, M.A. (1999). Regulation of the small GTP-binding protein Rho by cell adhesion and the cytoskeleton. EMBO J. *18*, 578–585.
41. Krendel, M., Zenke, F.T., and Bokoch, G.M. (2002). Nucleotide exchange factor GEF-H1 mediates cross-talk between microtubules and the actin cytoskeleton. Nat. Cell Biol. *4*, 294–301.